RESEARCH ARTICLE

Preparation and evaluation of $Zn_2(BDC)_2(DABCO)$ MOF-hydroxyapatite nanocomposite to remove tetracycline from aqueous solution

***Zainab Qutbi*[1], *Negar Motakef-Kazemi*[2,*], *Ensieh Ghasemi*[1]**

[1] *Department of Chemistry, Faculty of Pharmaceutical Chemistry, Tehran Medical Sciences, Islamic Azad University, Tehran, Iran*

[2] *Department of Medical Nanotechnology, Faculty of Advanced Sciences and Technology, Tehran Medical Sciences, Islamic Azad University, Tehran, Iran*

ARTICLE INFO

Article History:
Received 16 Aug 2024
Accepted 11 Oct 2024
Published 01 Dec 2024

Keywords:
Hydroxyapatite
Metal-organi framework
Nanocomposite
Tetracycline
Zn2(BDC)$_2$(DABCO)

ABSTRACT

Objective(s): In recent years, porous materials have shown good potential for adsorption due to their high surface area. Among them, hydroxyapatite (HA) is important as an inorganic material. While metal-organic frameworks (MOFs) have attracted much attention as hybrid materials consisting of organic and inorganic compounds with special properties

Methods: In this study, $Zn_2(BDC)_2(DABCO)$ MOF-HA nanocomposite (NC) was prepared by solvothermal method with precursors that are: Zn = zinc acetate dehydrates, BDC=1,4-benzenedicarboxylate, and DABCO=1,4-diazabicyclo [2.2.2] octane. This nanostructure was used to remove tetracycline drug from aqueous solution. Samples were characterized by Fourier Transform InfraRed (FTIR) spectroscopy to evaluate functional groups, X-Ray diffraction (XRD) analysis of crystal structure, field emission scanning electron microscope (FESEM) to determine morphology and size, BET analysis for measurement of surface area, and Ultraviolet–Visible (UV–Vis) spectroscopy to study drug adsorption. The effect of some important parameters on removal efficiency, such as drug concentration, nanocomposite amount, removal time and solution pH were studied. In order to reach best removal condition, the effect of the parameters and their interactions was optimized using the Box-Behnken Design (BBD) and the response surface methodology.

Results: The synthesis of $Zn_2(BDC)_2(DABCO)$ MOF-hydroxyapatite nanocomposite was confirmed using identification methods. The functional groups, crystal structure and surface area were evaluated by FTIR, XRD and BET respectively. The nanoscale size was approved by FESEM. In the optimum condition, the removal efficiency more than 98% was obtained.

Conclusions: According to the results, MOF and its nanocomposite can be a good choice for tetracycline removal and have good potential for the development of different adsorbents.

How to cite this article
Qutbi Z., Motakef-Kazemi N., Ghasemi E. Preparation and evaluation of Zn2(BDC)$_2$(DABCO) MOF-hydroxyapatite nanocomposite to remove tetracycline from aqueous solution. Nanomed Res J, 2024; 9(4): 393-401. DOI: 10.22034/nmrj.2024.04.006

INTRODUCTION

MOFs, as a class of materials consisting of organic and inorganic compounds, play an important role [1]. The application of these materials has extended due to their special properties in various fields such as nanomedicine [2], hydrogen storage [3], catalyst [4, 5], luminescence [6], sensor [7], adsorbent [8], electronic [9], Raman scattering [10], ion exchange [11], solar energy [12], drug delivery [13], and antibacterial action [14]. $Zn_2(BDC)_2(DABCO)$ MOF is a metal-organic framework based on zinc cluster and ligand BDC and DABCO with potential for various applications

* Corresponding Author Email: *motakef@iaups.ac.ir*

[15]. MOFs are prepared via self-assembly of metal ions (or clusters) and ligands by methods such as solution [16], solvothermal [17], hydrothermal [18], mechanochemical [19], electrochemical [20], sonochemical [21], microwave [22], laser abrasion [23].

Hydroxyapatite is a porous mineral material with diverse applications [24]. In recent years, hydroxyapatite-based nanomaterials have been used for adsorption from aqueous solutions an inorganic, green and environmentally friendly adsorbent [25]. Hydroxyapatite can absorb by ion exchange reaction mechanisms, surface complexation and physical adsorption such as electrostatic interaction and hydrogen bonding. Therefore, today it is important to expand the use of this compound [25, 26].

Antibiotic drugs as emerging pollutants as a result of widespread use cause environmental pollution and danger to humans and ecosystems [27, 28]. Treatment methods include advanced oxidation processes (photolysis, ozone, and photocatalytic/UV-based degradation), membrane filtration, reverse osmosis, and absorption [29]. The research on how to remove them from aqueous solutions through adsorbents by available and inexpensive compounds is very important [30, 31]. Surface adsorption of tetracycline is a common practice at the industrial level, especially in wastewater treatment processes [32]. Nowadays, nanostructures have a good potential to remove antibiotics due to their high surface area [33]. Today, nano adsorbents such as nanoparticles [34], silica nanotubes [35], carbon nanostructures [36, 37], nanofibers [38], MOFs [39, 40], hydroxyapatites [41, 42], and composites [42] have good potential for absorbing tetracycline antibiotics due to their high surface area. The aim is to prepare $Zn_2(BDC)_2(DABCO)$ MOF-hydroxyapatite nanocomposite as nano adsorbent to remove tetracycline from aqueous solution. Results show that the nanocomposite is a promising nanostructure to remove different pollutants form environment.

MATERIALS AND METHODS

Materials

All reagents with high purity and analytical grade were purchased from Merck (Darmstadt, Germany). Ultra-pure water was used for the preparation of all reagent solutions. Zinc acetate dehydrates ($Zn(Oac)_2.2H_2O$) salt, 1,4 benzenedicarboxylic acid ligand, 1,4-diazabicyclo [2.2.2] octane ligand, and dimethyl formamide (DMF) solvent were used for synthesis of $Zn_2(BDC)_2(DABCO)$ MOF. Hydroxyapatite was prepared from the Technical Research Campus of Yazd (Iran).

Preparation

For preparation of $Zn_2(BDC)_2(DABCO)$ MOF, the solvothermal method was used by adding Zn $(OAc)_2.2H_2O$ (0.132 g, 2 mmol) to the production of Zn^{2+} ions as a connector, BDC (0.1 g, 2 mmol) as a chelating ligand, and DABCO (0.035 g, 1 mmol) as a bridging ligand to 25 mL DMF as a solvent. The precursors were sealed under reflux and stirred at 90 °C for 15 min. Then, the reaction mixture was cooled to room temperature and filtered. The white crystals were washed with DMF to remove any metal and ligands that remained and dried in a vacuum for faster drying. DMF was removed from white crystals with a vacuum furnace at 150 °C for 5 h [43].

For preparation of $Zn_2(BDC)_2(DABCO)$ MOF-hydroxyapatite nanocomposite, metal precursor solution (zinc acetate 0.132 g) was mixed with 15 ml of dimethylformamide to 0.05 g of hydroxyapatite for 15 min, ligand precursor solution containing 0.1 g of BDC and 0.035 g DABCO was added with 10 ml of dimethylformamide solvent. Then it was rotated at 90 °C for 15 min. Then the product was centrifuged and washed twice with dimethylformamide solvent. Then it was placed in an oven at a temperature of 90 °C to dry the sediment. Finally, the deposit was placed in the furnace at a temperature of 120-150 °C for 5 h. Finally, the product is obtained.

Characterization

The samples were characterized by FTIR, XRD, FESEM, BET, and UV–vis spectroscopy. Fourier transform infrared spectra were recorded on a Spectrum Two spectrometer (PerkinElmer, Perkin Elmer Spectrum two, Germany) in a KBr matrix. X-ray diffraction measurements were performed using a X' Pert Pro diffractometer (Panalytical X'Pert Pro, Panalytical, Germany) for evaluation of crystalline structure. The morphology of nanocomposites was recorded by size field emission scanning electron microscope (TESCAN Vega3 Model, TESCAN, Czech). The surface area was evaluated by Brunauer–Emmett–Teller, BET, (Belsorp mini, Belsorp, Japan). UV–

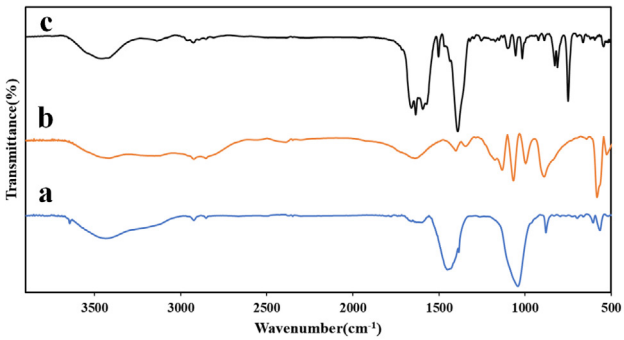

Fig. 1. FTIR spectra of a) MOF, b) HA, and c) MOF-HA NC

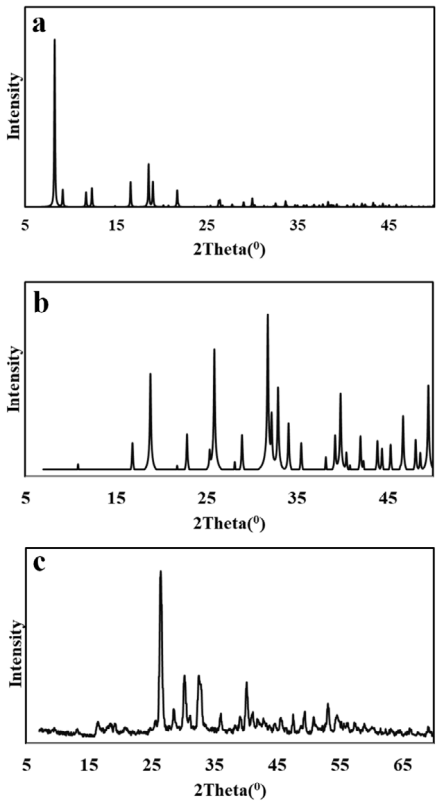

Fig. 2. XRD patterns of a) MOF, b) HA, and c) MOF-HA NC

Vis spectroscopy was done for investigation optic properties (Lambda25, Perkin Elmer, America).

RESULTS AND DISCUSSION

FTIR

FTIR spectra of samples were recorded in the range of 400–4000 cm^{-1} (Fig. 1). For MOF, the peak at ~3400 cm^{-1} is assigned C–H aromatic bands. The peak at ~2900 cm^{-1} is reported aliphatic C–H asymmetric stretching vibration. The peak at ~2600 cm^{-1} is assigned O–H...O valance stretching vibration band. The peak at ~1635 cm^{-1} is reported C=O stretching. The peak at ~1600 cm^{-1} is assigned aromatic C=C stretching [43]. For HA, the peak at ~3300 cm^{-1} is related to the O-H bond. The peak in the range of 1000 and 600 cm^{-1} indicates carbonate (CO_3^{-2}) and phosphate (PO_4^{3-}), respectively [44]. Based on FTIR results, peaks are observed in the nanocomposite.

XRD

X-ray diffraction patterns of samples were recorded from 2θ=5° to 80° (Fig. 2). The XRD

patterns show the crystalline structure based on previous report for MOF [43] and HA [44]. Based on the results, the characteristic peaks of MOF and HA were observed in the final nanocomposite.

FESEM

Field emission scanning electron microscope was used to evaluate the size and morphology of the samples (Figs. 3). Based on the results, MOF

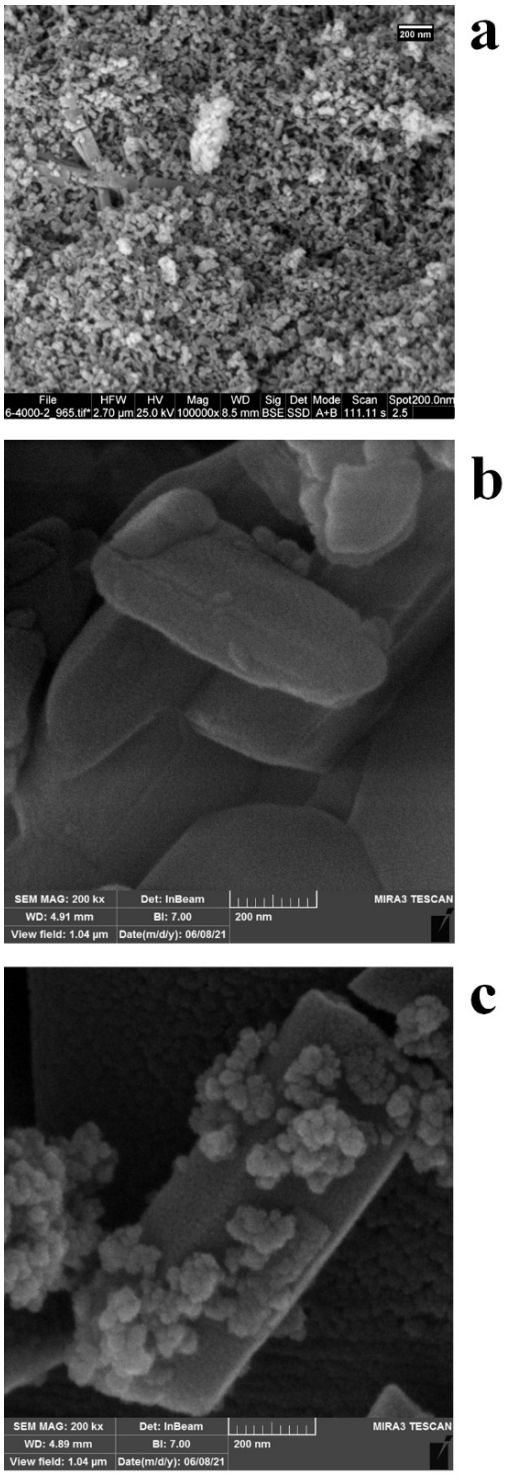

Fig. 3. FESEM images of a) MOF, b) HA, and c) MOF-HA NC

with nanometer scale is placed on hydroxyapatite. Based on the results, spherical nanoparticles with an average size of 100 nm and rod-shaped nanostructures with an average diameter of 150 nm were observed. MOF and HA nanostructures are observed in the final nanocomposite.

BET

The surface area of sample is measured by N_2 adsorption using BET analyses. Based on the results, the specific surface area is 1931.3 and 244.74 $m^2 g^{-1}$ for MOF and MOF-HA NC, respectively. The results are based on the IUPAC classification, type II isotherm curve for $Zn_2(BDC)_2(DABCO)$ and are in accordance with the previous report [45]. The reduction in surface area in the final nanocomposite is observed due to the presence of hydroxyapatite.

UV–vis spectroscopy

The amount of adsorbent was investigated at 0.15, 0.1, and 0.05 g (Fig. 5). Based on the results, the drug removal rate increased with increasing the amount of adsorbent. The results are consistent with the previous report and the removal rate increased with increasing MOF [46].

The tetracycline concentration was investigated at 0.15, 0.1, and 0.05 g (Fig. 6). Based on the results, the drug removal rate increased with decreasing drug concentration. The results are consistent with the previous report and the removal rate decreased with increasing concentration [46].

pH was investigated at 3, 6 and 9 (Fig. 7). Positive or negative charges are created on the surface of the environment by changing the pH of the solution. Based on the results, the drug removal rate increased with increasing pH because higher pH caused more active sites and reduced the competition between positive charges. Increase in pH and OH^- concentration gradually increases drug removal rate. The results were reported for the

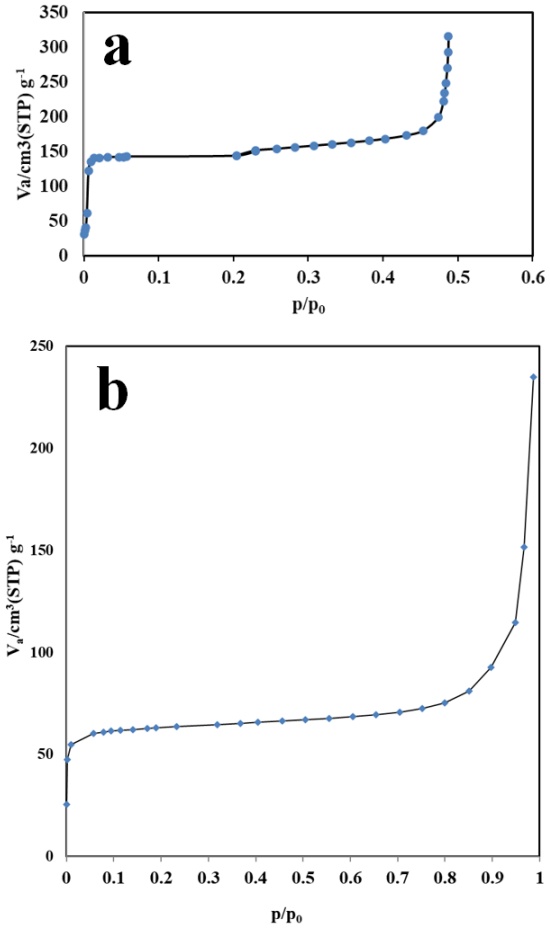

Fig. 4. Nitrogen isotherm of a) MOF and b) MOF-HA NC

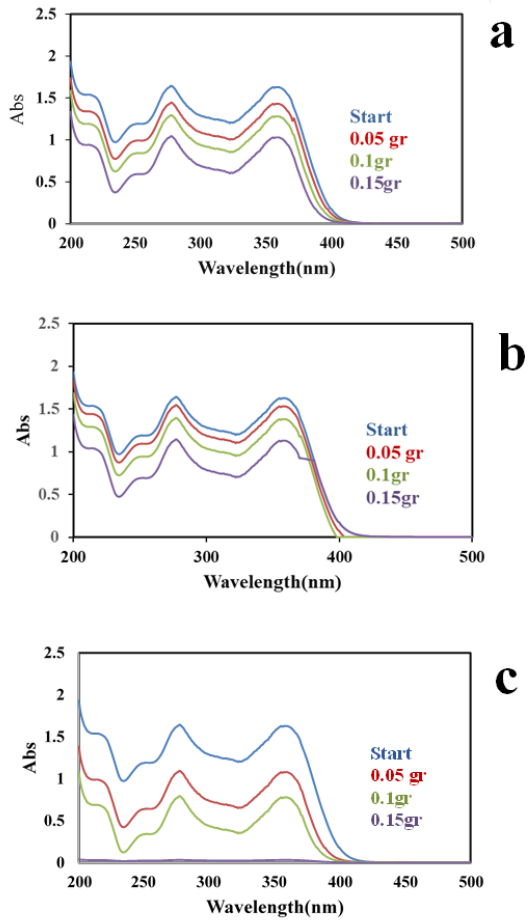

Fig. 5. Effect of adsorbent on drug removal rate by a) MOF, b) HA, and c) MOF-HA NC

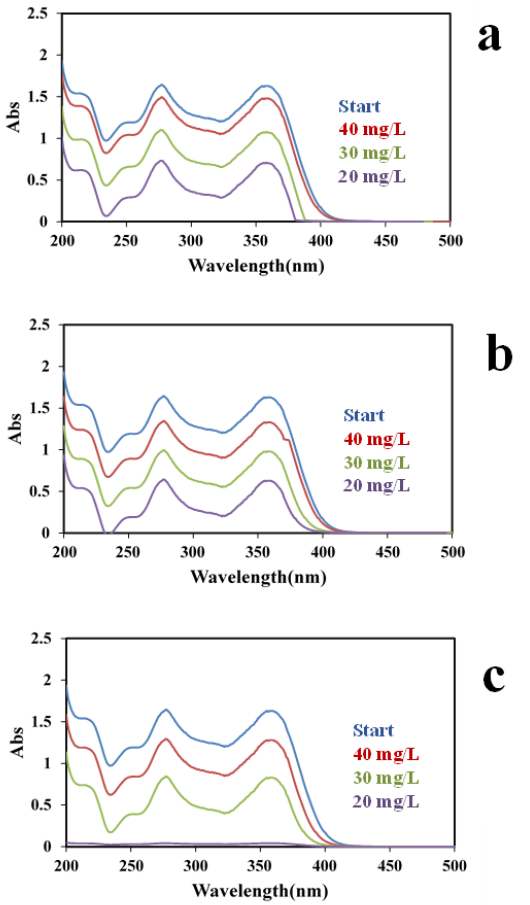

Fig. 6. Effect of drug concentration on drug removal rate by a) MOF, b) HA, and c) MOF-HA NC

first time.

The time was investigated at 30, 60, and 120 min (Fig. 8). Based on the results, the drug removal rate increased with time, which is consistent with the previous report [46].

Box-Behnken Design

In this study, for investigation and optimization of probable effective parameters, The Box–Behnken design (BBD) was performed. The BBD has been applied on fifteen randomized runs (2 × 3 (3-1) + 3 center points), by the STATGRAPHICS software. In addition, for finding the optimal point, a second-order polynomial model was fitted to correlate relationship between independent variables and response (removal efficiency%).

This design permitted the response to be modelled by fitting a second-order polynomial, which can be expressed as the following equation:

$$Y=\beta_0 + \beta_1 x_1 + \beta_2 x_2 + \beta_3 x_3 + \beta_{12} x_1 x_2 + \beta_{13} x_1 x_3 + \beta_{23} x_2 x_3 + \beta_{11} x_1^2 + \beta_{22} x_2^2 + \beta_{33} x_3^2$$

where x_1, x_2 and x_3 are the independent variables, b_0 is an intercept, β_1, β_2, β_3, β_{12}, β_{13}, β_{23}, β_{11}, β_{22} and β_{33} are the regression coefficients and Y is the response function (Removal efficiency%).

The quality of fit of the polynomial model equation was expressed by the coefficient of determination R^2. This equation has a determination coefficient (R^2) of 98.21%, indicating that only 1.79% of the total variations were not explained by the model.

The 3D response surface plots corresponding to the desirability function and their related counters for the removal efficiency are shown in Fig. 9. As it is shown in this figure, the removal efficiency is increased by increasing of pH. As it was demonstrated, more active sites are formed

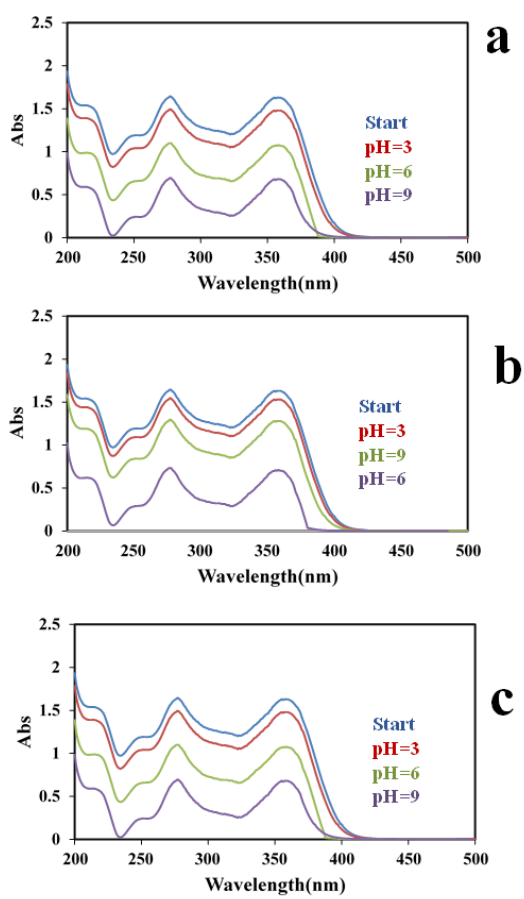

Fig. 7. Effect of pH on drug removal rate by a) MOF, b) HA, and c) MOF-HA NC

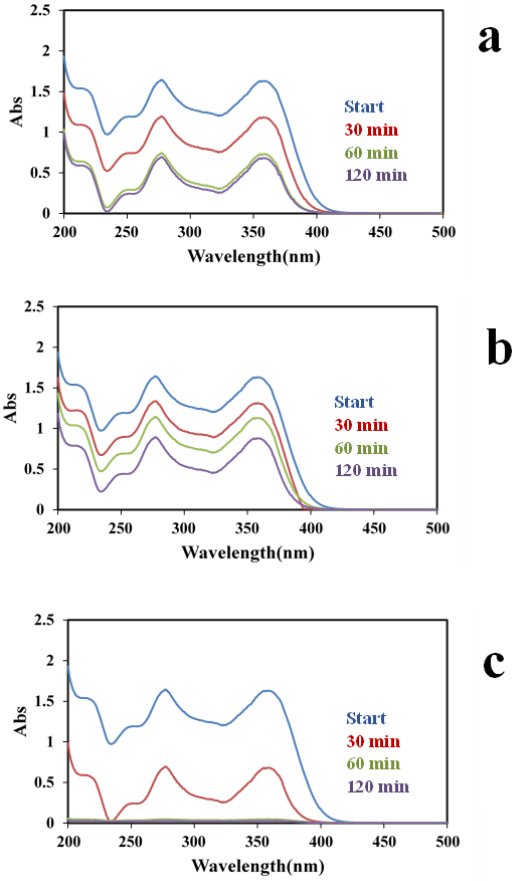

Fig. 8. Effect of time on drug removal rate by a) MOF, b) HA, and c) MOF-HA NC

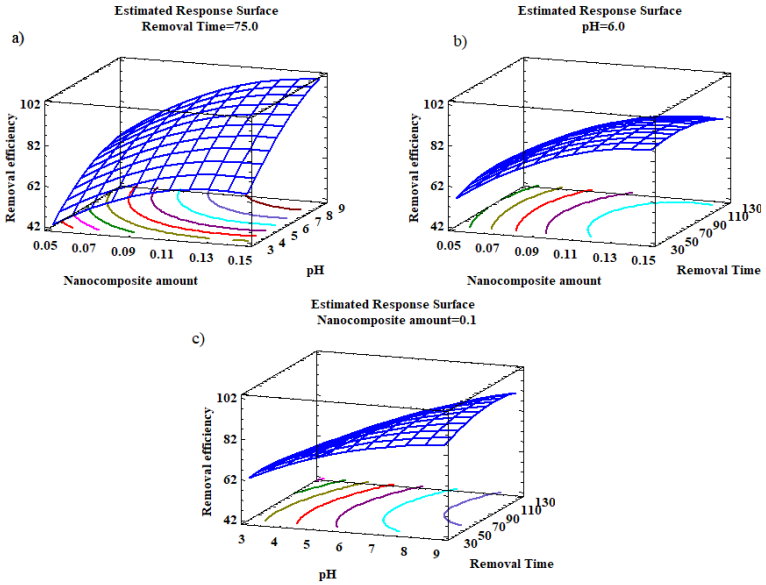

Fig. 9. The 3D response surface plots and corresponding contour plots for dye removal efficiency; a) nanocomposite amount and pH, b) nanocomposite amount and removal time, and c) pH and removal time, with related contours

in higher pH that caused to increase tetracycline removal efficiency.

Figure 9b shows the response surface obtained by plotting the nanocomposite amount versus the removal time. As can be seen in Fig. 9B and C, the results indicated that the removal efficiency increased by elevating the removal time to 60 min, and then decrease gradually. Also, as it is shown, increasing the amount of nanocomposite up to 0.12 g caused to increase the removal efficiency, and then remained almost constant. It seems that by increasing the nanocomposite concentration, the available surface area and adsorption sites are increased. According to the overall result of the optimization study, the following experimental conditions were chosen: pH 9; nanocomposite amount of 0.121 g and, adsorption time of 60 min. The results are consistent with the previous report [47].

CONCLUSION

The main objective of this study was to synthesis a novel and efficient $Zn_2(BDC)_2(DABCO)$ MOF-hydroxyapatite nanocomposite and then investigate its removal potential for tetracycline removal from aqueous samples. MOFs are porous materials that are of interest in various fields, especially in the field of pollutant removal. In this research, MOF-HA and nanocomposite were synthesized and characterized. The results of FTIR spectra confirm that the compounds were correctly synthesized. Examining the XRD patterns of all the samples shows that the crystalline structure is preserved in the samples. SEM results showed that the particle distribution of all samples is almost uniform. The results showed that the MOF in the form of a nanocomposite increased the removal rate. The experimental parameters such as the nanocomposite amount, solution pH and removal time were optimized using a BBD and the response surface methodology. Under optimized condition, the removal efficiencies were obtained more that 98%. The $Zn_2(BDC)_2(DABCO)$ MOF-hydroxyapatite nanocomposite has good application prospects for removal. Based on the results, the final nanocomposite based on metal-organic framework can have different applications.

CONFLICT OF INTEREST

The authors declare that there are no conflicts of interest.

REFERENCES

1. Zhu QL, Xu Q. Metal-organic framework composites. Chem Soc Rev. 2014;43:5468-512. https://doi.org/10.1039/C3CS60472A
2. Liu Y, Zhao Y, Chen X. Bioengineering of metal-organic frameworks for nanomedicine. Theranostics. 2019;9(11):3122-33. https://doi.org/10.7150/thno.31918
3. Shet SP, Priya SS, Sudhakar K, Tahir M. A review on current trends in potential use of metal-organic framework for hydrogen storage. Int J Hydrogen Energy. 2021;46(21):11782-803. https://doi.org/10.1016/j.ijhydene.2021.01.020
4. Gangu KK, Jonnalagadda SB. A review on metal-organic frameworks as congenial heterogeneous catalysts for potential organic transformations. Front Chem. 2021;9:747615. https://doi.org/10.3389/fchem.2021.747615
5. Alhumaimess MS. Metal-organic frameworks and their catalytic applications. J Saudi Chem Soc. 2020;24(6):461-73. https://doi.org/10.1016/j.jscs.2020.04.002
6. Gupta G, Thakur A. A comprehensive review on luminescent metal-organic framework detectors. Mater Today. 2022;50(5):1721-5. https://doi.org/10.1016/j.matpr.2021.09.170
7. Kreno LE, et al. Metal-organic framework materials as chemical sensors. Chem Rev. 2012;112(2):1105-25. https://doi.org/10.1021/cr200324t
8. Rani L, et al. A critical review on recent developments in MOF adsorbents for the elimination of toxic heavy metals from aqueous solutions. Environ Sci Pollut Res Int. 2020;27:44771-96. https://doi.org/10.1007/s11356-020-10738-8
9. Stavila V, Talin AA, Allendorf MD. MOF-based electronic and opto-electronic devices. Chem Soc Rev. 2014;43:5994-6010. https://doi.org/10.1039/C4CS00096J
10. Sun H, et al. Metal-organic frameworks as surface enhanced Raman scattering substrates with high tailorability. J Am Chem Soc. 2019;141:870-8. https://doi.org/10.1021/jacs.8b09414
11. Vilela SMF, et al. Multifunctionality in an ion-exchanged porous metal-organic framework. J Am Chem Soc. 2021;143(3):1365-76. https://doi.org/10.1021/jacs.0c10421
12. Chen B, et al. Emerging applications of metal-organic frameworks and derivatives in solar cells: Recent advances and challenges. Mater Sci Eng R Rep. 2023;152:100714. https://doi.org/10.1016/j.mser.2022.100714
13. Mallakpour S, Nikkhoo E, Hussain CM. Application of MOF materials as drug delivery systems for cancer therapy and dermal treatment. Coord Chem Rev. 2022;451:214262. https://doi.org/10.1016/j.ccr.2021.214262
14. Wyszogrodzka G, et al. Metal-organic frameworks: mechanisms of antibacterial action and potential applications. Drug Discov Today. 2016;21(6):1009-18. https://doi.org/10.1016/j.drudis.2016.04.009
15. Ryzhikov MR, Kozlova SG. Interactions between building blocks of the Zn2(BDC)2DABCO metal-organic framework. J Struct Chem. 2020;61:161-5. https://doi.org/10.1134/S0022476620020018
16. Tranchemontagne DJ, Hunt JR, Yaghi OM. Room temperature synthesis of metal-organic frameworks: MOF-5, MOF-74, MOF-177, MOF-199, and IRMOF-0. Tetrahedron. 2008;64:8553-7. https://doi.org/10.1016/j.tet.2008.06.036

17. Li Y, et al. Synthesis and shaping of metal-organic frameworks: a review. Chem Commun. 2022;58:11488-506. https://doi.org/10.1039/D2CC04190A
18. Sattar T, Athar M. Hydrothermal synthesis and characterization of copper glycinate (Bio-MOF-29) and its in vitro drugs adsorption studies. J Inorg Chem. 2017;7(2):17-27. https://doi.org/10.4236/ojic.2017.72002
19. Wang Z, Li Z, Ng M, Milner PJ. Rapid mechanochemical synthesis of metal-organic frameworks using exogenous organic base. Dalton Trans. 2020;49:16238-44. https://doi.org/10.1039/D0DT01240H
20. Al-Kutubi H, et al. Electrosynthesis of metal-organic frameworks: challenges and opportunities. ChemElectroChem. 2015;2(4):462-74. https://doi.org/10.1002/celc.201402429
21. Son WJ, Kim J, Kim J, Ahn WS. Sonochemical synthesis of MOF-5. Chem Commun. 2008;(47):6336-8. https://doi.org/10.1039/b814740j
22. Wang Y, et al. Microwave hydrothermally synthesized metal-organic framework-5 derived C-doped ZnO with enhanced photocatalytic degradation of rhodamine B. Langmuir. 2020;36(33):9658-67. https://doi.org/10.1021/acs.langmuir.0c00395
23. Ribeiro EL, et al. Laser-induced synthesis of ZIF-67: a facile approach for the fabrication of crystalline MOFs with tailored size and geometry. Mater Chem Front. 2019;3:1302-9. https://doi.org/10.1039/C8QM00671G
24. Haider A, et al. Recent advances in the synthesis, functionalization and biomedical applications of hydroxyapatite: a review. RSC Adv. 2017;7:7442-58. https://doi.org/10.1039/C6RA26124H
25. Balasooriya IL, et al. Applications of nano hydroxyapatite as adsorbents: A review. Nanomaterials. 2022;12(14):2324. https://doi.org/10.3390/nano12142324
26. Halim NAA, Hussein MZ, Kandar MK. Nanomaterials-upconverted hydroxyapatite for bone tissue engineering and a platform for drug delivery. Int J Nanomedicine. 2021;16:6477-96. https://doi.org/10.2147/IJN.S298936
27. Larsson DGJ, Flach CF. Antibiotic resistance in the environment. Nat Rev Microbiol. 2022;20:257-69. https://doi.org/10.1038/s41579-021-00649-x
28. Kraemer SA, Ramachandran A, Perron GG. Antibiotic pollution in the environment: From microbial ecology to public policy. Microorganisms. 2019;7(6):180. https://doi.org/10.3390/microorganisms7060180
29. Gopal G, et al. A review on tetracycline removal from aqueous systems by advanced treatment techniques. RSC Adv. 2020;10:27081-95. https://doi.org/10.1039/D0RA04264A
30. Eniola JO, Kumar R, Barakat MA. Adsorptive removal of antibiotics from water over natural and modified adsorbents. Environ Sci Pollut Res Int. 2019;26:34775-88. https://doi.org/10.1007/s11356-019-06641-6
31. Ferchichi K, et al. Low-cost posidonia oceanica bio-adsorbent for efficient removal of antibiotic oxytetracycline from water. Environ Sci Pollut Res Int. 2022;29(55):83112-25. https://doi.org/10.1007/s11356-022-21647-3
32. Swapna Priya S, Radha KV. A review on the adsorption studies of tetracycline onto various types of adsorbents. Chem Eng Commun. 2017;204(8):821-39. https://doi.org/10.1080/00986445.2015.1065820
33. Malakootian M, Yaseri M, Faraji M. Removal of antibiotics from aqueous solutions by nanoparticles: a systematic review and meta-analysis. Environ Sci Pollut Res Int. 2019;26(9):8444-58. https://doi.org/10.1007/s11356-019-04227-w
34. Debnath B, et al. The effective adsorption of tetracycline onto zirconia nanoparticles synthesized by novel microbial green technology. J Environ Manage. 2020;261:110235. https://doi.org/10.1016/j.jenvman.2020.110235
35. Althumayri K, et al. Enhanced adsorption and evaluation of tetracycline removal in an aquatic system by modified silica nanotubes. ACS Omega. 2023;8(7):6762-77. https://doi.org/10.1021/acsomega.2c07377
36. Yang J, et al. Effectively removing tetracycline from water by nanoarchitecture carbons derived from CO2: Structure and surface chemistry influence. Environ Res. 2021;195:110883. https://doi.org/10.1016/j.envres.2021.110883
37. Yu F, Ma J, Han S. Adsorption of tetracycline from aqueous solutions onto multi-walled carbon nanotubes with different oxygen contents. Sci Rep. 2014;4:5326. https://doi.org/10.1038/srep05326
38. Lu L, et al. Effective removal of tetracycline antibiotics from wastewater using practically applicable iron(III)-loaded cellulose nanofibers. R Soc Open Sci. 2021;8:210336. https://doi.org/10.1098/rsos.210336
39. Abbasnia A, et al. Removal of tetracycline antibiotics by adsorption and photocatalytic-degradation processes in aqueous solutions using metal organic frameworks (MOFs): A systematic review. Inorg Chem Commun. 2022;145:109959. https://doi.org/10.1016/j.inoche.2022.109959
40. Beiranvand M, Farhadi S, Mohammadi-Gholami A. Adsorptive removal of tetracycline and ciprofloxacin drugs from water by using a magnetic rod-like hydroxyapatite and MIL-101(Fe) metal-organic framework nanocomposite. RSC Adv. 2022;12(53):34438-53. https://doi.org/10.1039/D2RA06213E
41. Oliveira C, et al. Zinc (II) modified hydroxyapatites for tetracycline removal: Zn (II) doping or ZnO deposition and their influence in the adsorption. Polyhedron. 2021;194:114879. https://doi.org/10.1016/j.poly.2020.114879
42. Ersan M, et al. Synthesis of hydroxyapatite/clay and hydroxyapatite/pumice composites for tetracycline removal from aqueous solutions. Process Saf Environ Prot. 2015;96:22-32. https://doi.org/10.1016/j.psep.2015.04.001
43. Motakef-Kazemi N, Asadi A. Methylene blue adsorption from aqueous solution using Zn2(Bdc)2(Dabco) metal-organic framework and its polyurethane nanocomposite. Iran J Chem Chem Eng. 2022;41(12):3950-62.
44. Gheisari H, Karamian E, Abdellahi M. A novel hydroxyapatite-Hardystonite nanocomposite ceramic. Ceram Int. 2015;41(4):5967-75. https://doi.org/10.1016/j.ceramint.2015.01.033
45. Rahmani F, et al. Synthesis of Zn2(BDC)2(DABCO) metal-organic framework and its polyethylene glycol composite for acetaminophen delivery. Iran J Sci. 2024;48:397-407. https://doi.org/10.1007/s40995-023-01544-1
46. Wei F, et al. The application of bimetallic metal-organic frameworks for antibiotics adsorption. J Saudi Chem Soc. 2022;26(6):101562. https://doi.org/10.1016/j.jscs.2022.101562
47. Ghourchian F, et al. Zn-based MOF-chitosan-Fe3O4 nanocomposite as an effective nano-catalyst for azo dye degradation. J Environ Chem Eng. 2021;9(6):106388. https://doi.org/10.1016/j.jece.2021.106388